AIP | Applied Physics Letters

The Boersch effect in a picosecond pulsed electron beam emitted from a semiconductor photocathode

Makoto Kuwahara, Yoshito Nambo, Kota Aoki, Kensuke Sameshima, Xiuguang Jin, Toru Ujihara, Hidefumi Asano, Koh Saitoh, Yoshikazu Takeda, and Nobuo Tanaka

Citation: Applied Physics Letters **109**, 013108 (2016); doi: 10.1063/1.4955457
View online: http://dx.doi.org/10.1063/1.4955457
View Table of Contents: http://scitation.aip.org/content/aip/journal/apl/109/1?ver=pdfcov
Published by the AIP Publishing

The Boersch effect in a picosecond pulsed electron beam emitted from a semiconductor photocathode

Makoto Kuwahara,[1,2,a)] Yoshito Nambo,[2] Kota Aoki,[2] Kensuke Sameshima,[2] Xiuguang Jin,[3] Toru Ujihara,[1,2] Hidefumi Asano,[2] Koh Saitoh,[1,2] Yoshikazu Takeda,[4,5] and Nobuo Tanaka[1]
[1]*Institute of Materials and Systems for Sustainability, Nagoya University, Nagoya 464-8603, Japan*
[2]*Graduate School of Engineering, Nagoya University, Nagoya 464-8603, Japan*
[3]*High Energy Accelerator Research Organization (KEK), Tsukuba 305-0801, Japan*
[4]*Aichi Synchrotron Radiation Center, Seto 489-0965, Japan*
[5]*Nagoya Industrial Science Research Institute, Nagoya 460-0008, Japan*

(Received 14 March 2016; accepted 25 June 2016; published online 7 July 2016)

The space charge effect has been clearly observed in the energy distributions of picosecond pulse beams from a spin-polarized electron microscope, and was found to depend upon the quantity of charge per pulse. The non-linear phenomena associated with this effect have also been replicated in beam simulations that take into account of a three-dimensional space charge. The results show that a charge of 500 aC/pulse provides the highest brightness with a 16-ps pulse duration, a 30-keV beam energy, and an emission spot of 1.8 μm. Furthermore, the degeneracy of the wave packet of the pulsed electron beam has been evaluated to be 1.6×10^{-5} with a charge of 100 aC/pulse, which is higher than that for a continuously emitted electron beam despite the low beam energy of 30 keV. The high degeneracy and high brightness contribute to the realization of high temporal and energy resolutions in low-voltage electron microscopy, which will serve to reduce radiolysis damage and enhance scattering contrast. [http://dx.doi.org/10.1063/1.4955457]

Narrow energy spreads of electron beams contribute to higher energy resolution in electron energy-loss spectroscopy (EELS) and reduction of chromatic aberration.[1] Such energy spreads are also important for the temporal coherence of an electron wavepacket.[2] A narrow electron beam linewidth is usually realized using a monochromatic filter applied to the illumination system of a transmission electron microscope (TEM).[3] The narrowest achieved energy spread of 9 meV has been demonstrated by combining a cold field emission gun and an alpha-type monochromator, which improved the energy resolution of the EELS and allowed the observation of phonon scattering with fast electrons.[4] A spin-polarized electron beam emitted from a semiconductor photocathode with a negative electron affinity surface also has a narrow linewidth due to the extraction process.[5] A narrow linewidth of 112 meV with a high wavepacket degeneracy of 1.6×10^{-6} results in high brightness and long temporal coherence simultaneously, meaning that the brightness in a certain energy window is higher than that in a cold field emitter.[6]

In contrast, a time-resolved measurement in electron microscopy is realized by an ultrashort-pulse electron beam, which can be used to obtain not only real space images and EELS but also reciprocal space information.[7–12] Stroboscopic detection in the time-resolved measurement is usually applied to reversible phenomena due to the necessities of reliability and precise repetition. In the case of irreversible phenomena, e.g., structure changing, bond breaking, or phase transitions, a single-shot imaging technique is used to capture a moment in the course of these reactions.[13,14] In the single-shot imaging process, the amount of charge in a pulse is important for ensuring fast temporal resolution and sufficient image contrast. However, the space charge effect suppresses the amount of charge due to the repulsive Coulomb force under high charge density, which makes the spread wider in both transverse and longitudinal momentum space.[15–17] Specifically, the broadening of the energy spread is termed the Boersch effect, which leads to the degradation of the energy resolution and an increase in chromatic aberration.[18]

Pulse beam emission and measurements of the energy distributions were conducted in a spin-polarized TEM (SP-TEM) with an ultrashort-pulse laser. The cathode used was a semiconductor photocathode, which had a GaAs-GaAsP-strained superlattice structure in the active layer, to control the spin polarization and the temporal structure of the emitted electron beam. The photocathode had a maximum polarization of about 90% at a wavelength of 780 nm due to the selective excitation of spin-polarized electrons at the bandgap energy of 1.58 eV.[19] A drive laser with a diameter of 1.8 μm was focused on the photocathode surface. The pulsed electron beam emitted from the photocathode surface was accelerated to a voltage of 30 kV over a traveled distance of 8 mm.[20] The pulsed laser had a central wavelength of 780 nm, 99% circular polarization, a repetition frequency of 80 MHz, and a 16-ps pulse duration created by selecting out a wavelength from a femtosecond mode-locked laser to reduce the bandwidth of the frequency and broaden the pulse duration.[21] The intensity of the pulse laser was tuned continuously by a polarized beam splitter and a half-wave plate. The pulse duration of the laser was measured by optical interferometric autocorrelation with a non-linear crystal.

[a)]kuwahara@imass.nagoya-u.ac.jp

In contrast, the pulse duration of the electron beam was measured by a combination of ultrafast electric deflectors and an imaging sensor, which allowed the temporal space to be converted into position space.[22,23] The energy distributions of the electron pulse beams were measured by an electron energy spectrometer equipped downstream of the electron beam trajectory of the TEM.

The energy distribution of the pulsed electron beam was investigated for different charge quantities with a laser pulse duration of 16 ps, which is a significant specification for time-resolved (TR) TEM and TR-EELS. The charge of each electron pulse was set to range from 10 aC to 10 fC by tuning the power of the drive laser. For each charge value, the energy distribution was measured by the energy spectrometer with an exposure time of 1 s, over which 8×10^7 pulses occurred. Figure 1 shows the energy spectrum of the pulsed electron beam for several charge series; for a small charge of 10 aC/pulse, the energy spread had a full width at half maximum (FWHM) of only 0.4 eV. The narrow energy spread obtained with the picosecond pulse duration could realize a high energy resolution and a high temporal resolution simultaneously in TR-EELS. The result also demonstrates that the photocathode could generate a high-charge density electron beam (e.g., 10 fC/pulse) with a tiny emission spot size of 1.8 μm.

However, as the charge was increased, the energy spread of the electron beam was observed to broaden. Additionally, the central peak was separated into two peaks. Finally, for the 10 fC/pulse, the energy spread increased to an FWHM of 20 eV. Figure 2 shows the energy width of the pulsed electron beam as a function of the charge per pulse. The increment in energy space reveals a non-linear correlation with the charge, which is a clear demonstration of the Boersch effect. The broadening of the energy spread did not depend on the number of cross-over points of the accelerated electron beam. Therefore, the Boersch effect mainly occurs in the acceleration region between the photocathode and the anode.[5]

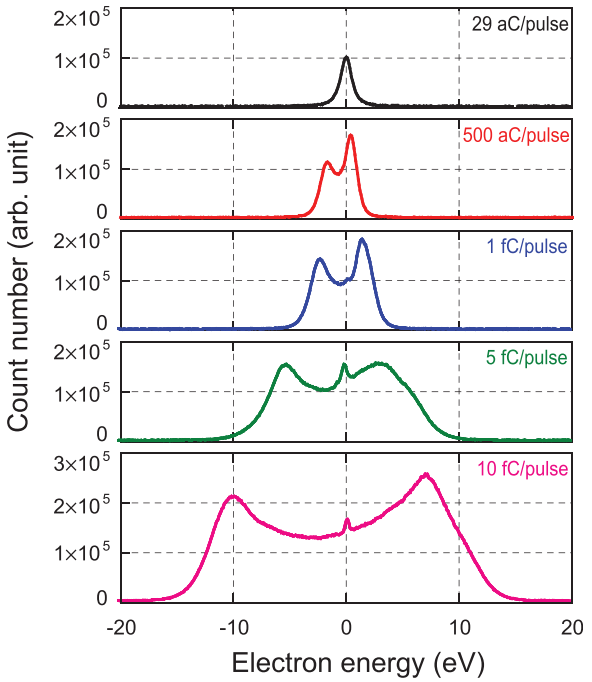

FIG. 1. The experimental results for the electron energy distribution for several charge quantities per pulse as a function of the electron energy. The vertical axis indicates the electron count number measured by an imaging sensor. The horizontal axis indicates the difference from the central beam energy of 30 keV.

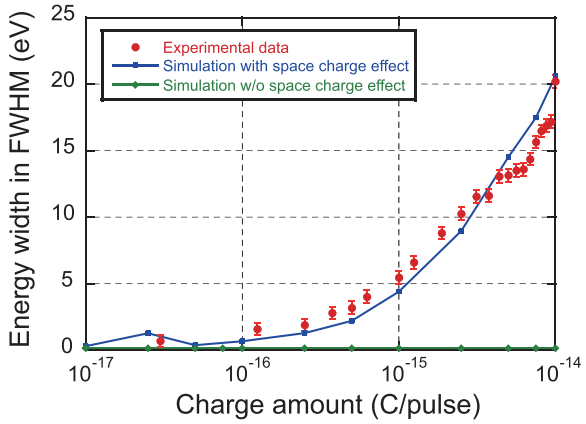

FIG. 2. The energy width of a pulsed electron beam as a function of the quantity of charge per pulse. The vertical axis indicates the energy width at full width at half maximum (FWHM) of the electron count number as measured by an imaging sensor. The red circles with error bars show the experimental data. The blue and green solid lines show the simulation data with and without taking into account the space charge effect, respectively.

An electron beam simulation revealed that the charge-dependence of the energy width broadening is due to the space charge effect. The simulation was used to investigate the non-linear effect of the energy spread broadening in a region of high charge, taking into account the space charge effect and an actual electric field in the electron gun of the SP-TEM. The simulation code used was *General Particle Tracer*, based on a charged particle model. The simulation results are presented in Fig. 2 as solid colored lines. The blue and green solid lines show simulated energy widths with and without the space charge effect, respectively. Figure 3(a) shows the charge series of the evaluated energy distributions in real space after a

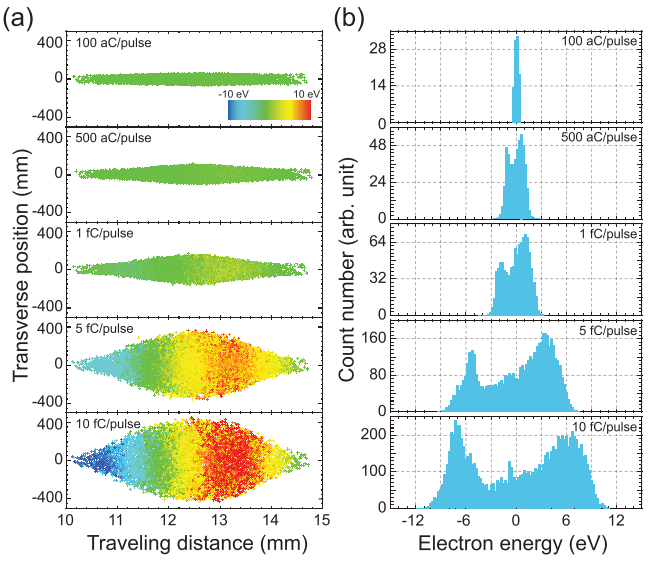

FIG. 3. (a) Particle distributions in the real space of a simulated pulse electron beam. The color mapping indicates the energy difference from the central beam energy. (b) The simulated energy spectrum converted from part (a) of the figure as a function of the electron energy, shown as difference from the central beam energy of 30 keV. The vertical axis shows the count number for individual electron energies.

250-ps travel time from the photocathode surface. The color indicates the beam energy separation from the central beam energy in each macroparticle. The transverse beam size also grew at the center as the charge increased. The higher-energy part of the forward region of the electron beam pulse was accelerated by the repulsive force of Coulomb interaction, and vice versa. Figure 3(b) shows the energy spectrum propagated from the data of Fig. 3(a) in comparison with the experimental spectrum of Fig. 1. The energy distribution supports the features of the experimental data and the two peaks created by the repulsive force due to the space charge effect. It appears that there is a trade-off relation between high-contrast single-shot TEM imaging and the high energy resolution of EELS.

To determine the appropriate conditions for TR-TEM and TR-EELS, the brightness and degeneracy of an electron wave packet were examined. Brightness is a useful parameter not only for adjusting the image contrast of TEM but also for extracting phase information. Moreover, the degeneracy is the filling rate of quantum coherence volume per cell volume h^3 in a phase space consisting of three real spaces and three momentum spaces; degeneracy is a significant parameter for the brightness of a monochromated electron beam and intensity interference. The brightness of the pulsed electron beam is described as

$$B = \left(\gamma^2 - 1\right)\frac{eN}{\epsilon_{nx}\epsilon_{ny}\tau} = \left(\gamma^2 - 1\right)B_n, \tag{1}$$

where N and e are the electron number and electron charge, ϵ_{nx} and ϵ_{ny} are the normalized emittances in Cartesian coordinates, and τ and γ are the temporal width of a pulse beam and a Lorentz factor, respectively. B_n is a normalized brightness that does not depend on the beam energy.[24] The degeneracy is defined as

$$\delta = \frac{h^3 N}{2\epsilon_{nx}\epsilon_{ny}\epsilon_{nz}\left(m_0 c\right)^3}, \tag{2}$$

where h and m_0 are the Planck's constant and electron mass, respectively. ϵ_{nz} is the normalized emittance in the longitudinal direction; if the normalized longitudinal-emittance, ϵ_{nz}, is equivalent to $\tau\Delta E/(m_0 c)$, where ΔE is the energy spread of an electron beam, degeneracy δ can be described as $B_n h^3/(e m_0^2 c^2 \Delta E)$. Note that the degeneracy is proportional to the brightness per electron energy spread.[6]

Figure 4 shows the charge-dependence of the brightness at a beam energy of 30 keV, as well as the degeneracy calculated by the simulation code for a charged particle model involving the space charge effect. The brightness increases with the charge; however, the relation between the brightness and charge is non-linear in the high-charge region because of the degradation of the transverse emittance due to the repulsive force (the transverse space charge effect). The brightness has broad peak at around 500 aC/pulse. In contrast, the degeneracy also has a peak at 100 aC/pulse, which is lower than that associated with the brightness. The peak shift between the brightness and the degeneracy is due to the degradation of the energy spread compared with that of the transverse space charge effect, which occurs strongly even in low-charge regions. The abrupt decrease in the region above 60 fC/pulse is caused by a long pulse length in the longitudinal direction that

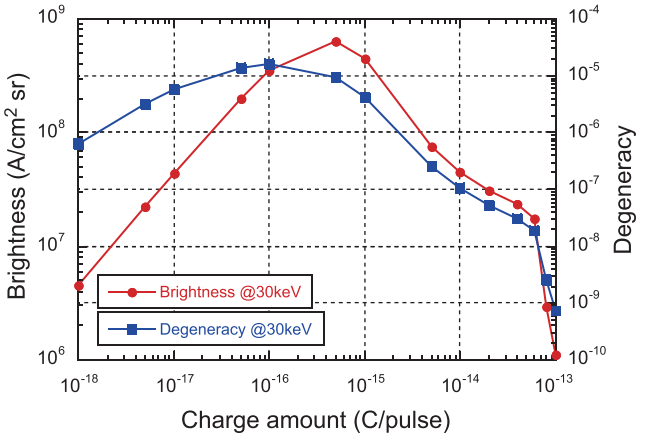

FIG. 4. The brightness and degeneracy of a wave packet with a 16-ps pulse duration and a 30-keV beam energy at 250 ps after electron emission from the photocathode surface as a function of the amount of charge per pulse.

is longer than the acceleration space due to the strong repulsive force. The use of the highest degeneracy is appropriate for TR-EELS in single-shot imaging or the generation of a monochromated probe beam. The figure also shows that the pulsed TEM can provide a highest degeneracy of 1.6×10^{-5} at 100 aC/pulse, which is higher than that for a cold field-emission source under continuous operation.[25,26] This highly degenerate wave packet is effective for an intensity-interference experiment in SP-TEM, because an anti-bunching effect in the second-order correlation function depends on the degeneracy and the spin polarization.[6] Furthermore, a pulsed electron beam in SP-TEM with regular repetition will increase the signal-to-noise ratio due to a reduction in the noise level of non-counting intervals.[21,22] The spin-polarized electrons extracted from a semiconductor photocathode with a negative electron affinity surface have sufficient coherence to provide first-order interference and are expected to generate a second-order interference because of their high degeneracy.

The non-linear phenomena associated with the longitudinal space charge effect (Boersch effect) have been clarified by quantitative evaluation and comparison with simulated energy distributions. The highest possible brightness of the pulsed electron beam, which can be used to achieve a short exposure time or a small cumulative number of shots for multiple-shot imaging in pump-probe measurements, was also estimated. The shortened acquisition time suppressed some problems with mechanical instabilities and time jitter between the pump laser and probe beam, leading to a more precise measurement in terms of both temporal and spatial resolution. The brightness per unit energy was also evaluated using the degeneracy of the wave packet in pulse operation, which allowed determination of the most appropriate conditions for TR-EELS with a monochromatic filter. It was revealed that an improvement in the degeneracy could be realized by the pulse operation. The high brightness and high degeneracy of a pulsed electron beam with a low beam energy of 30 keV will contribute not only to time-resolved imaging but also to higher scattering contrasts and reductions in radiolysis damage in analytical methods using electron probe beams.[27]

The authors thank Dr. H. Shinada, Dr. M. Koguchi, Dr. M. Tomita, Dr. M. Sugaya, and Dr. A. Furukawa of Hitachi

Central Research Laboratory for their helpful supports and encouragements. This research was supported by JSPS KAKENHI Grant Nos. 25706031 and 15K13404.

[1]L. Reimer and H. Kohl, *Transmission Electron Microscopy*, 5th ed. (Springer, New York, 2008), p. 38.
[2]A. H. Zewail and M. Thomas, *4D Transmission Electron Microscopy* (Inperial College Press, London, 2009), p. 167.
[3]K. Kimoto, Microscopy **63**, 337–344 (2014).
[4]O. L. Krivanek, T. C. Lovejoy, N. Dellby, T. Aoki, R. W. Carpenter, P. Rz, E. Soignard, J. Zhu, P. E. Batson, M. J. Lagos, R. F. Egerton, and P. A. Crozier, Nature **514**, 209–212 (2014).
[5]M. Kuwahara, S. Kusunoki, Y. Nambo, K. Saitoh, X. G. Jin, T. Ujihara, H. Asano, Y. Takeda, and N. Tanaka, Appl. Phys. Lett. **105**, 193101 (2014).
[6]M. P. Silverman, Phys. Lett. A **120**, 442 (1987).
[7]R. M. van der Veen, O.-H. Kwon, A. Tissot, A. Hauser, and A. H. Zewail, Nat. Chem. **5**, 395–402 (2013).
[8]L. Piazza, D. J. Masiel, T. LaGrange, B. W. Reed, B. Barwick, and F. Carbone, Chem. Phys. **423**, 79–84 (2013).
[9]A. Feist, E. Echternkamp, J. Schauss, S. V. Yalunin, S. Schafar, and C. Roper, Nature **521**, 200–203 (2015).
[10]R. J. D. Miller, Science **343**, 1108–1116 (2014).
[11]S. Tokita, M. Hirokane, M. Murakami, S. Shimizu, M. Hashida, and S. Sakabe, Phys. Rev. Lett. **105**, 215004 (2010).
[12]Y. Murooka, N. Naruse, S. Sakakihara, M. Ishimaru, J. Yang, and K. Tanimura, Appl. Phys. Lett. **98**, 251903 (2011).
[13]J. E. Evans and N. D. Browning, Microscopy **62**, 147–156 (2013).
[14]L. Nikolova, M. J. Stem, J. M. MacLeod, B. W. Reed, H. Ibrahim, G. H. Campbell, F. Rosei, T. LaGrange, and B. J. Siwick, J. Appl. Phys. **116**, 093512 (2014).
[15]B. J. Siwick, J. R. Dwyer, R. E. Jordan, and R. J. D. Miller, J. Appl. Phys. **92**, 1643 (2002).
[16]M. R. Armstrong, K. Boyden, N. D. Browning, G. H. Campbell, J. D. Colvin, W. J. DeHope, A. M. Frank, D. J. Gibson, F. Hartemann, J. S. Kim, W. E. King, T. B. LaGrange, B. J. Pyke, B. W. Reed, R. M. Shuttlesworth, B. C. Stuart, and B. R. Torralva, Ultramicroscopy **107**, 356 (2007).
[17]T. van Oudheusden, E. F. de Jong, S. B. van der Geer, W. P. E. M. Op't Root, O. J. Luiten, and B. J. Siwick, J. Appl. Phys. **102**, 093501 (2007).
[18]H. Boersch, Z. Phys. **139**, 115 (1954).
[19]X. G. Jin, N. Yamamoto, Y. Nakagawa, A. Mano, T. Kato, M. Tanioku, T. Ujihara, Y. Takeda, S. Okumi, M. Yamamoto, T. Nakanishi, T. Saka, H. Horinaka, T. Kato, T. Yasue, and T. Koshikawa, Appl. Phys. Express **1**, 045002 (2008).
[20]M. Kuwahara, S. Kusunoki, X. G. Jin, T. Nakanishi, Y. Takeda, K. Saitoh, T. Ujihara, H. Asano, and N. Tanaka, Appl. Phys. Lett. **101**, 033102 (2012).
[21]Y. Nambo, M. Kuwahara, S. Kusunoki, K. Sameshima, K. Saitoh, T. Ujihara, H. Asano, Y. Takeda, and N. Tanaka, AMTC Lett. **4**, 256 (2014), available at http://amtc5.com/imges/file/vol4/amtc_4_123.pdf.
[22]Y. Honda, S. Matsuba, X. G. Jin, T. Miyajima, M. Yamamoto, T. Uchiyama, M. Kuwahara, and Y. Takeda, Jpn. J. Appl. Phys. **52**, 086401 (2013).
[23]K. Aulenbacher, J. Schuler, D. V. Harrach, E. Reichert, J. Röthgen, A. Subashev, V. Tioukine, and Y. Yashin, J. Appl. Phys. **92**, 7536–7543 (2002).
[24]P. W. Hawkes and H. Kasper, *Principles of Electron Optics* (Academic Press, London, 1989), Vol. 2, Chap. 48.
[25]H. Kiesel, A. Renz, and F. Hasselbach, Nature **418**, 392 (2002).
[26]T. Kodama, N. Osakabe, J. Endo, A. Tonomura, K. Ohbayashi, T. Urakami, S. Ohsuka, H. Tsuchiya, Y. Tsuchiya, and Y. Uchikawa, Phys. Rev. A **57**, 2781 (1998).
[27]R. F. Egerton, Ultramicroscopy **145**, 85 (2014).